Sensor-Based Predictive Communication for Highly Dynamic Multi-Hop Vehicular Networks

Roman Alieiev*, Jiri Blumenstein†, Roman Maršalek†, Thorsten Hehn*, Andreas Kwoczek*, Thomas Kürner‡
*Group Research, Volkswagen AG, Wolfsburg, Germany
†The Faculty of Electrical Engineering and Communication, Brno University of Technology, Czech Republic
‡Institut für Nachrichtentechnik, Technische Universität Braunschweig, Braunschweig, Germany
*{roman.alieiev, thorsten.hehn, andreas.kwoczek}@volkswagen.de,
†{blumenstein, marsaler}@feec.vutbr.cz, ‡kuerner@ifn.ing.tu-bs.de

***Abstract*—We introduce a sensor-aided predictive algorithm for multi-hop link quality estimation. The proposed concept uses vehicle sensor data to improve a link adaptation and end-to-end path selection for a vehicular multi-hop data transmission. The obtained results show that the proposed concept allows better multi-hop link quality estimation and significantly improves end-to-end transmission characteristics in dynamic vehicular environments.**

I. Introduction

The process of driving tasks automation and vehicle-to-vehicle (V2V) communications have become key trends in shaping automotive industry of the future. These technological advances combined with various types of mission critical and functional safety applications impose high requirements on the quality of the end-to-end communication between vehicles [1]. However, high dynamics of vehicles, acting as communicating partners, combined with unique properties of vehicular environment such as an impact of Doppler effects, presence of scatterers at both sides of the communication link pose a range of distinct link quality estimation challenges compared to existing cellular-based solutions.

In wireless communications, the optimal transmission scheme is adaptively selected based on the estimated channel state information (CSI). The time required for CSI estimation and dynamics of the channel eventually result in a selection of a suboptimal data transmission scheme and in an overall network performance degradation, also known as CSI aging [2].

The problem of channel estimation and optimal end-to-end path selection in dynamic multi-hop networks is even more challenging. A large number of possible links and hops to be monitored by a decision making node results in an increased mismatch between the estimated and actual CSI at the transmission time.

The importance of minimizing CSI aging is a recognized problem in literature [3]. It has been also shown [4] that technological achievements of modern vehicles lead by developments in automated driving solutions can be beneficially used to improve communication between two vehicles due to a better understanding of the nature of communication link properties. The benefits of sensor-aided prediction for direct link vehicular communications were highlighted in [5]. To the best of our knowledge, existing works do not address the the possibility of applying sensor-based vehicular prediction algorithms for a multi-hop link quality forecasting and an end-to-end path selection in highly dynamic vehicular networks.

In current work we extend the concept of sensor-aided predictive communications, originally developed for a direct-link [5], to a multi-hop V2V scenarios. The *key contributions* of this paper are:

- We evaluate the benefit of sensor-based predictive communications in vehicular multi-hop link-quality-estimation tasks,
- We present different ways how the concept of predictive communication can be applied to multi-hop V2V,
- We verify the applicability of the proposed approach via simulation in a select vehicular scenario with realistic sensors and environment properties.

II. The problem of channel state information aging

In this section we highlight the problem of an CSI aging in direct-link and multi-hop vehicular communications.

Let us consider a multi-hop decode-and-forward V2V communication environment. Due to high dynamics of vehicles, surrounded by other objects, the communication link between two partners experiences time-varying large and small scale fading effects. We also assume each relay to employ the single carrier frequency division multiplexing (SC-FDM) with the LTE-A uplink reference symbol structure and a Zero-forcing (ZF) equalization strategy [6].

A. Single-hop CSI aging

Given the aforementioned assumptions, a received symbol vector $\boldsymbol{y}$ at subcarrier k can be expressed as [7]

$$\boldsymbol{y}_k = \boldsymbol{H}_{k,k}\boldsymbol{W}_k\boldsymbol{s}_k + \sum_{k' \neq k} \boldsymbol{H}_{k,k'}\boldsymbol{W}_{k'}\boldsymbol{s}_{k'} + \boldsymbol{n}_k, \qquad (1)$$

where $\boldsymbol{H}_{k,k'} \in \mathbb{C}^{N_r \times N_t}$ is a channel matrix for N_t transmit and the N_r receive antennas between k-th and k'-th subcarrier, $\boldsymbol{W}_k \in \mathbb{C}^{N_t \times N_l}$ is an N_l-layer precoding matrix at k-th subcarrier, and $\boldsymbol{s}_k \in \mathbb{C}^{N_l}$ is a vector of data symbols with σ_s^2 being the average power transmitted on each layer. The component $\sum_{k' \neq k} \boldsymbol{H}_{k,k'}\boldsymbol{W}_{k'}\boldsymbol{s}_{k'}$ represents the impact of the so-called Inter-Carrier Interference (ICI) with the power σ^2_{ICI},

ISBN 978-0-9928626-7-1

and $\boldsymbol{n} \in \mathbb{C}^{N_r}$ denotes zero mean additive white Gaussian noise with variance σ_n^2 on antenna n_r.

Since the pilot symbols are separated in time, the time-varying nature of the channel results in an inevitable channel estimation error between the true channel $\boldsymbol{H}$ and the estimated channel $\hat{\boldsymbol{H}}$ at data positions:

$$\boldsymbol{E} = \boldsymbol{H} - \hat{\boldsymbol{H}}, \tag{2}$$

with σ_e^2 being the mean squared error (MSE) at each element.

Inserting (1) into (2) and denoting $\boldsymbol{e}_{s_k} = \boldsymbol{s}_k - \hat{\boldsymbol{s}}_k$, where $\hat{\boldsymbol{s}}_k$ is the ZF estimate of $\boldsymbol{s}_k$, we compute the layer-dependent symbol estimation MSE covariance matrix [7]:

$$MSE = \mathbb{E}\left\{\boldsymbol{e}_{s_k}\boldsymbol{e}_{s_k}^{\mathrm{H}}\right\} = (\sigma_n^2 + \sigma_{\mathrm{ICI}}^2 + \sigma_e^2\sigma_{\mathrm{d}}^2)\hat{\boldsymbol{\Psi}} \tag{3}$$

where σ_{d} is data symbol power and $\hat{\boldsymbol{\Psi}} \in \mathbb{C}^{N_l \times N_l}$ is the inverse of squared estimated effective channel.

From (3) the following estimated signal-to-interference-plus-noise ratio (SINR) at m-th layer is defined [6]:

$$\hat{\gamma}_m = \frac{\sigma_s^2}{(\sigma_n^2 + \sigma_{\mathrm{ICI}}^2 + \sigma_e^2\sigma_{\mathrm{d}}^2)\hat{\psi}_m}, \tag{4}$$

with $\hat{\psi}_m$ being m, m-th element of $\hat{\boldsymbol{\Psi}}$.

Additionally we assume that precoded symbols are transmitted in blocks using a set of M modulation and coding schemes (MCS), $C = \{C_1, C_2, \ldots, C_M\}$, characterized by SINR thresholds S and spectral efficiencies R. The block is assumed to be transmitted efficiently if the estimated SINR $\hat{\gamma}_m$ exceeds the threshold S_j with the selected MCS index j.

Due to channel aging, the actual link quality may deviate from underestimated $\hat{j} < j$ or overestimated $\hat{j} > j$ applied MCS indexes. In the latter case the link will not be able to successfully transmit data and will need an additional time for the failure detection, MCS reconfiguration and data retransmission. As a result, in both cases the the spectral efficiency of the link becomes underutilized.

B. Multi-hop CSI aging

The problem of delayed channel feedback is even more significant in dynamic multi-hop vehicular environments.

To highlight the problem, let us consider a SISO-based multi-hop communication, where the **end-to-end link selection and resource allocation** is done at the node initiating the transmission, denoted as $\mathcal{A}$. Also each node is only capable to signal pilot symbols for channel quality estimation only within its scheduled resource blocks. In this case the *end-to-end multi-hop feedback delay* will have twofold contributions. On one hand, estimation of a reliable CSI-feedback at each link takes time:

$$d_{\mathrm{link}} = k_{\mathrm{avg}} \cdot d_{\mathrm{ps}}, \tag{5}$$

where d_{ps} is a time interval between two consecutive pilot symbols and k_{avg} is a number of consecutive channel estimations needed to obtain reliable channel feedback.

On the other hand the maximum network-relevant delay $d_{\mathrm{nr,est}}(\mathcal{N})$ between a specific node $\mathcal{N}$ and the decision making node $\mathcal{A}$ is caused by a periodicity of feedback reports d_{pFB} to the decision making node, time per each hop $i_{\mathcal{N}}$ to deliver $d_{\mathrm{d},i_{\mathcal{N}}}$ and process $d_{\mathrm{pr},i_{\mathcal{N}}}$ the channel relevant information over $I_{\mathcal{N}}$ hops between $\mathcal{A}$ and $\mathcal{N}$:

$$d_{\mathrm{nr,est}}(\mathcal{N}) = d_{\mathrm{pFB}} + \sum_{i_{\mathcal{N}}=1}^{I_{\mathcal{N}}} (d_{\mathrm{d},i_{\mathcal{N}}} + d_{\mathrm{pr},i_{\mathcal{N}}}), \tag{6}$$

Finally, the vector of maximum feedback delays for the shortest path between the decision making node and each of L nodes of interest will depend on vectors of scheduled feedback periodicities $\boldsymbol{d}_{\mathrm{pFB}}$ and multi-hop feedback delivery times:

$$\boldsymbol{d}_L = k_{\mathrm{avg}} d_{\mathrm{ps}} + \boldsymbol{d}_{\mathrm{pFB}} + \begin{bmatrix} \sum_{i_1=1}^{I_1} (d_{\mathrm{d},i_1} + d_{\mathrm{pr},i_1}) \\ \sum_{i_2=1}^{I_2} (d_{\mathrm{d},i_2} + d_{\mathrm{pr},i_2}) \\ \cdots \\ \sum_{i_L=1}^{I_L} (d_{\mathrm{d},i_L} + d_{\mathrm{pr},i_L}) \end{bmatrix}. \tag{7}$$

After the required CSI-information has been received by the decision making node, the *path selection* and *resource allocation* process will be affected by feedback delays $\boldsymbol{d}_L$.

In contrast to the path selection and resource allocation, the efficiency of the actual **end-to-end data transmission** at any given link B between node $\mathcal{N}$ and its direct neighbor will be also affected by the maximum delay $d_{\mathrm{nr,est}}(\mathcal{N})$ to deliver and process CSI feedback from $\mathcal{N}$ to $\mathcal{A}$ plus the additional delay to deliver and process data from $\mathcal{A}$ to $\mathcal{N}$ over $I_{\mathcal{N}}$ links:

$$d_{\mathrm{nr,data}}(\mathcal{N}) = d_{\mathrm{nr,est}}(\mathcal{N}) + \sum_{i_{\mathcal{N}}=1}^{I_{\mathcal{N}}} (d_{\mathrm{d},i_{\mathcal{N}}} + d_{\mathrm{pr},i_{\mathcal{N}}}). \tag{8}$$

Finally, the dynamics of the SINR aging compared to actual SINR $\gamma(B)$ for the fixed path at a given link B will be

$$a_\gamma(B) = \frac{\gamma(B) - \hat{\gamma}(B)}{d_{\mathrm{nr,data}}(\mathcal{N})}. \tag{9}$$

Based on (4), (7) and (8), the resulting impact of CSI-aging on an end-to-end link efficiency in a multi-hop network will be characterized by the following parameters:

- applied channel estimation techniques
- relation between the dynamics of the link quality change and the feedback delay
- statistical distribution of the feedback delays
- applied method of the feedback delivery
- ability to predict the expected CSI state

III. Sensor-based prediction for multi-hop communications

The need for channel prediction to compensate a feedback delay is a known problem [3]. Existing approaches collect multiple past channel estimates to predict future channel conditions [8]. Nevertheless, most of them are application- or scenario-limited. For example, the performance of spline interpolation and averaging highly depends on the dynamics of environment, while historical averaging fails completely in dynamic environments with direct link communications [8].

ISBN 978-0-9928626-7-1 © EURASIP 2017

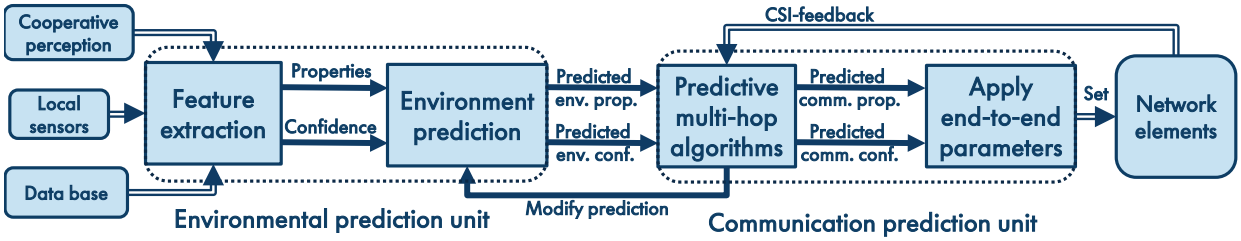

Fig. 1. Block-scheme of the sensor-based multi-hop predictive vehicular communication

A. Sensor-based prediction in V2V communications

Recently it has been shown, that the ability of vehicles to collect surrounding information via on-board sensors brings unique context-aware advantages for direct V2V communications [5]. In this paper we extend the sensor-based prediction scheme to the multi-hop vehicular communication according to Fig. 1 and evaluate corresponding applicability regions.

Let us assume a sensor-equipped vehicle capable to fuse available sensor data, process it and conduct feature extraction. This information can be transferred to the communication system, which will learn about the vehicle's position, dynamics, presence of objects with distinct properties and will enable estimation of expected environmental states. Since the exchange of local information about environment is the inherent property of V2V communications, we assume that each vehicle is capable to obtain dynamic and static properties of the surrounding environment including other vehicles with the precision of the available off-the-shelf sensor equipment.

Let us further assume a V2V network with M vehicles involved in multi-hop communication tasks, as shown in Fig. 2. We further assume that the information about environment is periodically exchanged among the vehicles. Finally at the time instant t the following processed information will be available at the decision making node:

- a vector of M estimated positions and directions $\hat{\boldsymbol{p}}_{\mathrm{vh}}$ combined with absolute velocities of each vehicle $\hat{\boldsymbol{v}}_{\mathrm{dv}}$,
- a matrix of estimated positions $\hat{\boldsymbol{P}}_{\hat{O}}$ and estimated dimensions $\hat{\boldsymbol{D}}_{\hat{O}}$ of $\hat{O}$ detected scattering objects,
- a vector of delayed CSI-feedbacks $\boldsymbol{f}_{\mathrm{CSI}}(\gamma)$ from L scheduled links between M nodes,
- vectors of corresponding feedback delays $\boldsymbol{d}_L$ and data transmission delays $\boldsymbol{d}_{\mathrm{nr,data}}(\mathcal{N})$ defined in (7) and (8),
- a vector of confidence intervals for received feedback parameters, which depend on properties of detected objects.

Based on this information, a range of predictive algorithms can be realized at the decision making node by solving an optimization problem and applying a proper constraint. To mention a few: the minimization of the multi-hop CSI-aging impact, minimization of required feedback over the network, selection of the most efficient or stable end-to-end path, etc.

In the current work we limit our scope on applying the predictive multi-hop communication to minimize the impact of CSI-aging on the end-to-end data transmission efficiency between the decision making node $\mathcal{A}$ and the node $\mathcal{D}$.

Let us define the optimal efficiency at time t of the end-to-end transmission as the spectral efficiency $R_{j,D_{\mathrm{w}}}$ of the weakest link D_{w} between a node $\mathcal{D}_{\mathrm{w}-1}$ and $\mathcal{D}_{\mathrm{w}}$ which has the highest SINR out of all weakest links in all possible paths between $\mathcal{A}$ and $\mathcal{D}$. As it was discussed in Chapter II, the actually selected spectral efficiency for each link deviates from the optimal due to multi-hop CSI-aging. Then, if the end-to-end path was optimally selected and following (8), the *non-predictive* approach according to Section II-B results in the following SINR mismatch:

$$\Delta\gamma_{\mathcal{AD}}(D_{\mathrm{w}}) = a_{\gamma}(D_{\mathrm{w}})(d_{\mathrm{pFB}} + 2\sum_{i_{\mathcal{D}_{\mathrm{w}}}=1}^{I_{\mathcal{D}_{\mathrm{w}}}}(d_{\mathrm{d},i_{\mathcal{D}_{\mathrm{w}}}} + d_{\mathrm{pr},i_{\mathcal{D}_{\mathrm{w}}}})). \tag{10}$$

In contrary, for the *predictive* communication the following algorithm is applied at the decision making node, see Fig. 1:

1) based on available information about environment, such as $\hat{\boldsymbol{p}}_{\mathrm{vh}}$, $\hat{\boldsymbol{v}}_{\mathrm{dv}}$, $\hat{\boldsymbol{P}}_{\hat{O}}$, $\hat{D}_{\mathrm{O}}$, and received delayed CSI-feedbacks from each link of interest, predict the expected CSI-states and confidence intervals for every link d out of L at the time of potential link use,
2) find the optimal end-to-end path from $\mathcal{A}$ to $\mathcal{D}$ given the predicted CSI-states and confidence intervals,
3) start transmission and, if applicable, adjust feedback periodicity requests $d_{\mathrm{pFB,pred}}(\mathcal{D}_{\mathrm{w}}) = d_{\mathrm{pFB}} \cdot d_{\alpha(D_{\mathrm{w}})}$ according to coefficient $d_{\alpha(D_{\mathrm{w}})}$ dependent on prediction deviation parameter $\alpha(D_{\mathrm{w}})$,
4) adjust confidence intervals based on the new feedback.

Now the predictive SINR mismatch at the weakest link D_{w} depends on prediction deviation per unit of time $\alpha(D_{\mathrm{w}})$ and time $d_{\mathrm{pred}}(\mathcal{D}_{\mathrm{w}})$ to reach the link D_{w}, which is similar to the non-predictive $d_{\mathrm{nr,data}}(\mathcal{D})$ case but has variable feedback periodicity parameter $d_{\mathrm{pFB,pred}}(\mathcal{D}_{\mathrm{w}})$ instead of fixed $d_{\mathrm{pFB}}(\mathcal{D})$:

$$\Delta\gamma_{\mathrm{prd}}(D_{\mathrm{w}}) = \alpha(D_{\mathrm{w}})d_{\mathrm{pred}}(\mathcal{D}_{\mathrm{w}}). \tag{11}$$

Plugging (8) in (11) the expanded form will be:

$$\Delta\gamma_{\mathrm{prd}}(D_{\mathrm{w}}) = \alpha(D_{\mathrm{w}})(d_{\mathrm{pFB}}d_{\alpha(D_{\mathrm{w}})} + 2\sum_{i_{\mathcal{D}_{\mathrm{w}}}=1}^{I_{\mathcal{D}_{\mathrm{w}}}}(d_{\mathrm{d},i_{\mathcal{D}_{\mathrm{w}}}} + d_{\mathrm{pr},i_{\mathcal{D}_{\mathrm{w}}}})). \tag{12}$$

As can be seen from (12), the sensor-based predictive approach differs by the prediction deviation parameter $\alpha(D_{\mathrm{w}})$ and by the periodicity coefficient $d_{\alpha(D_{\mathrm{w}})}$.

ISBN 978-0-9928626-7-1 © EURASIP 2017

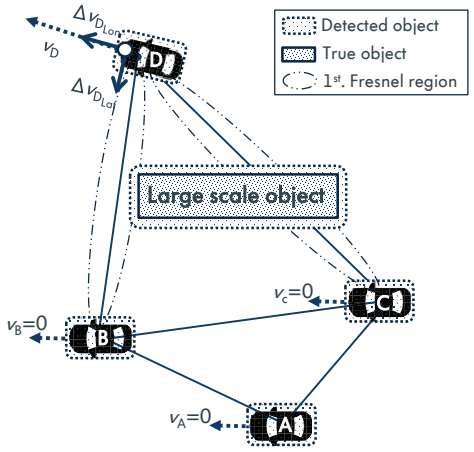

Fig. 2. An illustrative example of multi-hop V2V communication affected by the presence of an obstacle with a static sender node $\mathcal{A}$, two static relay nodes $\mathcal{B}$ and $\mathcal{C}$, and the highly dynamic receiving node $\mathcal{D}$

IV. Simulation and results

In this chapter we define the scenario of interest, describe the simulation setup and present and discuss obtained results.

A. Scenario definition

In order to conduct simulations we first consider the over-simplified configuration with only four vehicles involved in the communication, denoted as $\mathcal{A}$, $\mathcal{B}$, $\mathcal{C}$, $\mathcal{D}$, as shown in Fig. 2. We assume vehicle $\mathcal{A}$ to be a source, which collects CSI feedback, and vehicle $\mathcal{D}$ a sink of the multi-hop transmission, respectively, while $\mathcal{B}$ and $\mathcal{C}$ are possible relays. Further we assume only vehicle $\mathcal{D}$ to have non-zero velocity of $v_D = 55$ m/s and limit our setup to maximum allowed number of hops being two. We also assume that over the simulation time period the moving vehicle passes next to the obstacle which results in a sharp NLOS-to-LOS transition for the $\mathcal{B}$-$\mathcal{D}$ link.

B. Simulation setup

The simulation was conducted in two phases. First, the link level channel mismatch power levels σ_e^2 discussed in Section II-A were estimated for a typical range of absolute and relative velocities and typical link level channel conditions for the select scenario, namely *Highway: free flow* [9]. The initial simulations were performed in a Matlab-based **V2V link-level simulation environment**, which is developed from the Vienna LTE-A uplink simulator [10]. For this purpose a set of changes was introduced to reflect key properties of direct link V2V environment, for the link-level implementation details and simulation setup, see [5]. For all simulation scenarios we consider a 5.9 GHz carrier frequency, which results in the most challenging Doppler effects among widely used frequencies for V2V communications. Besides these modifications, we estimated the impact of Doppler effects on the SINR based on available sensor information and sensor accuracy [5].

After the link level properties for a select scenario were obtained, the results in terms of estimated mean squared error (MSE) powers σ_e^2 per Doppler shift, Rician K-factor[1] and sensor-accuracy were plugged into the specifically developed **large scale multi-hop simulation environment**. At this point the evolution of large scale parameters for each object was found. The distance dependent pathloss function for V2V Highway scenario defined in [11] was coupled with the impact of three largest Fresnel zones. Then the correlation properties of slow fading process were coupled with the select scenario properties and with an evolution of each link over space according to [12]. The prediction-relevant properties, such as velocity, positioning and object recognition error parameters are derived from the existing sensor-fusion solutions, available in [13]. Modifications of the simulator and key parameters of both simulation setups are summarized in Table I.

Setup for Simulation and Channel Model	
Antenna configuration	SISO
Tx and Rx ant. heights, [m]	$[1.5, 1.5]$
Type of a channel Model	Modified SCME [14]
Number of scenario realizations	100
NLOS-LOS transition time, [ms]	80
Carrier Frequency, [GHz]	5.9
Bandwidth, [MHz]	1.4
Access technique	SC-FDMA
Absolute velocity for $\mathcal{A}$, $\mathcal{B}$, $\mathcal{C}$, $\mathcal{D}$, [m/s]	$[0, 0, 0, 55]$
Slow fading, deviation [dB]	3
Slow fading, 90% correlation distance [m]	1.25
Tx power at each relay, [dBm]	23
Obstacle attenuation, [dB]	$[5 : 5 : 20]$
Mean position (x, y) error, $\boldsymbol{\mu}^{\Delta p}$	$[0, 0]$
Position error deviation, $\boldsymbol{\sigma}$	$[0.25, 0.5]$

TABLE I
Simulation setup

C. Simulation results

To highlight the benefit of predictive algorithms and to understand the regions of their applicability, in the **first simulation setup** we evaluate the network efficiency loss in terms of SINR mismatch between the actual value and the values available at node $\mathcal{A}$ via delayed CSI feedback of the weakest link over different levels of channel variations a_γ. For this purpose we fix the multi-hop path to be $\mathcal{A}$-$\mathcal{B}$-$\mathcal{D}$ and vary the steepness of the signal attenuation change by changing maximum NLOS attenuation level of the scatterer.

Two different configurations of CSI-feedback updates were considered in this setup: (a) non-predictive periodic CSI-feedback with maximum feedback delays set to $\boldsymbol{d}_{\text{pfb}} = [7, 27]$ ms; (b) predictive periodic CSI-feedback with positioning inaccuracy modeled by Gaussian process with deviation set to $\boldsymbol{\sigma} = [0.25, 0.5]$ m. In the latter case, the prediction and expected steepness of the SINR change for the NLOS-LOS transition of the weakest link is found based on difference between the actual SINR level at NLOS region and expected SINR at the time of LOS. The predicted SINR for the given link as well as the start and end of the NLOS-LOS transition is estimated based on sensor-aided information about environment, available at vehicles, as discussed in Section III-A.

[1]The ratio between the power of the specular and diffuse components.

ISBN 978-0-9928626-7-1 © EURASIP 2017

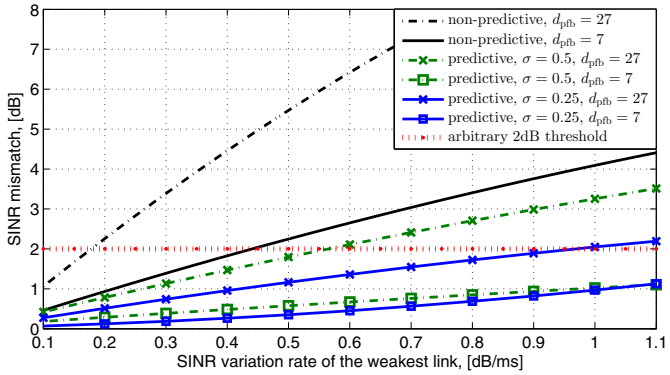

Fig. 3. Impact of the link variation rate on the SINR mismatch, when a multi-hop feedback is delayed. The link variation rate is defined as the SINR variation a rate of the weakest link in the multi-hop setup

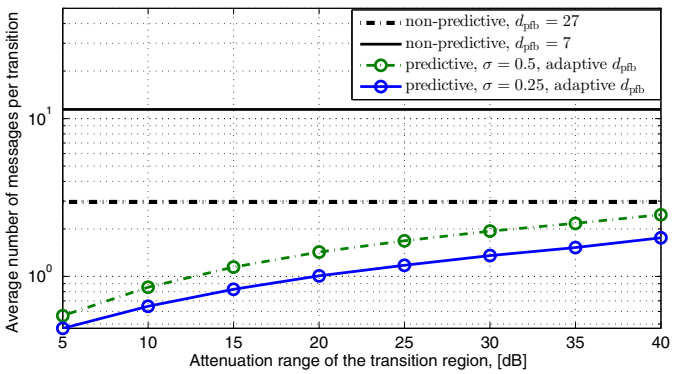

Fig. 4. Average number of feedback messages during NLOS-LOS transition. The transition region is defined by the range of attenuation change, which is the difference between maximum and minimum attenuation over the transition process

The results of this simulation setup are shown in Fig. 3. The predictive algorithm shows superior performance compared to the non-predictive algorithms. Additionally, it can be seen that position uncertainty of detected objects (vehicles and obstructing objects) influences the efficiency of predictive approach, while an increase in channel variations deteriorates performance of both algorithms.

In the **second simulation setup** we demonstrate how the predicted information about future CSI at each link reduces the number of feedback messages required to limit the SINR mismatch. For this purpose we consider a non-predictive case with periodic CSI-feedback as in the first simulation setup and predictive approach with the adaptive periodicity of the CSI-feedback generation $d_{\text{pfb,pred}}$, as described in Section III-A. First, the SINR mismatch at different levels of SINR variation rates are calculated for various possible feedback intervals, as described in the previous simulation setup. Then certain tolerable threshold is arbitrary selected based on allowed mean SINR mismatch. Finally, the predicted feedback periodicity is obtained from the intersecting point of the arbitrary threshold and one of feedback periodicity curves at position of the expected SINR variation rate. Fig. 3 illustrates the predictive selection of $d_{\text{pfb,pred}} = \{7, 27\}$ for the arbitrary threshold of 2 dB (which approximately corresponds to one MCS step). The simulation results presented in Fig. 4 show that predictive algorithms are capable to significantly reduce the number of CSI-feedback over the wide range of transition regions compared to non-predictive periodic CSI-feedback.

V. Conclusions and Future Work

We presented the concept of vehicle sensor-aided predictive link quality estimation for multi-hop V2V communications in dynamic environments. The obtained results show the applicability of the proposed concept in multi-hop V2V networks, where nodes are capable to obtain and exchange information about the surrounding environment. In future work, other road scenarios will be investigated. Besides this, further analysis of the impact of scattering reflections, and number of nodes on sensor-aided prediction in multi-hop transmission will be done.

References

[1] A. Sherer, J. Rose, and R. Oddone, "Ensuring functional safety compliance for ISO26262," in *2015 52nd ACM/EDAC/IEEE Design Automation Conference (DAC)*, June 2015, pp. 1–3.

[2] R. A. Akl, S. Valentin, G. Wunder, and S. Stanczak, "Compensating for cqi aging by channel prediction: The lte downlink," in *2012 IEEE Global Communications Conference (GLOBECOM)*, Dec 2012, pp. 4821–4827.

[3] A. Duel-Hallen, "Fading channel prediction for mobile radio adaptive transmission systems," *Proceedings of the IEEE*, vol. 95, no. 12, pp. 2299–2313, Dec 2007.

[4] R. C. Daniels and R. W. Heath, "Link adaptation with position/motion information in vehicle-to-vehicle networks," *IEEE Transactions on Wireless Communications*, vol. 11, no. 2, pp. 505–509, February 2012.

[5] R. Alieiev, T. Hehn, A. Kwoczek, and T. Kürner, "Sensor-based communication prediction for dynamic Doppler-shift compensation," in *Proceedings. (ITST 2017). International Conference on ITS Telecommunications*, IEEE, May 2017.

[6] A. Hedayat, A. Nosratinia, and N. Al-Dhahir, "Linear equalizers for flat rayleigh mimo channels," in *Proceedings. (ICASSP '05). IEEE International Conference on Acoustics, Speech, and Signal Processing, 2005.*, vol. 3, March 2005, pp. iii/445–iii/448.

[7] M. Šimko, Q. Wang, and M. Rupp, "Optimal pilot symbol power allocation under time-variant channels," *EURASIP Journal on Wireless Communications and Networking*, vol. 2012, no. 1, p. 225, 2012.

[8] T. Cui, F. Lu, V. Sethuraman, A. Goteti, S. P. Rao, and P. Subrahmanya, "First order adaptive iir filter for cqi prediction in hsdpa," in *2010 IEEE Wireless Communication and Networking Conference*, April 2010.

[9] L. Elefteriadou, "The highway capacity manual 6th edition: A guide for multimodal mobility analysis," *ITE Journal*, vol. 86, no. 4, 2016.

[10] J. Blumenstein, J. C. Ikuno, J. Prokopec, and M. Rupp, "Simulating the long term evolution uplink physical layer," in *ELMAR, 2011 Proceedings*. IEEE, 2011, pp. 141–144.

[11] A. F. Molisch, F. Tufvesson, J. Karedal, and C. F. Mecklenbräuker, "A survey on vehicle-to-vehicle propagation channels," *IEEE Wireless Communications*, vol. 16, no. 6, pp. 12–22, December 2009.

[12] A. Paier, J. Karedal, N. Czink, C. Dumard, T. Zemen, F. Tufvesson, A. F. Molisch, and C. F. Mecklenbräuker, "Characterization of vehicle-to-vehicle radio channels from measurements at 5.2 GHz," *Wireless Personal Communications*, vol. 50, no. 1, pp. 19–32, 2009.

[13] C. Merfels and C. Stachniss, "Pose fusion with chain pose graphs for automated driving," in *Proceedings of the IEEE/RSJ International Conference on Intelligent Robots and Systems (IROS)*, 2016.

[14] D. S. Baum, J. Hansen, and J. Salo, "An interim channel model for beyond-3G systems: extending the 3GPP spatial channel model (SCM)," in *2005 IEEE 61st Vehicular Technology Conference*, vol. 5, May 2005, pp. 3132–3136 Vol. 5.

ISBN 978-0-9928626-7-1 © EURASIP 2017